5-4-2012

Hormone-Induced 14-3-3γ Adaptor Protein Regulates Steroidogenic Acute Regulatory Protein Activity and Steroid Biosynthesis in MA-10 Leydig Cells

Yasaman Aghazadeh

Malena B. Rone

Josip Blonder

Xiaoying Ye

Timothy D. Veenstra
Cedarville University, tveenstra@cedarville.edu

See next page for additional authors

THE JOURNAL OF BIOLOGICAL CHEMISTRY VOL. 287, NO. 19, pp. 15380–15394, May 4, 2012
Published in the U.S.A.

Hormone-induced 14-3-3γ Adaptor Protein Regulates Steroidogenic Acute Regulatory Protein Activity and Steroid Biosynthesis in MA-10 Leydig Cells*

Received for publication, January 3, 2012, and in revised form, February 27, 2012 Published, JBC Papers in Press, March 16, 2012, DOI 10.1074/jbc.M112.339580

Yasaman Aghazadeh[‡1], Malena B. Rone[‡2], Josip Blonder[§], Xiaoying Ye[§], Timothy D. Veenstra[§], D. Buck Hales[¶], Martine Culty[‡‖], and Vassilios Papadopoulos[‡‖3]**

*From [‡]The Research Institute of the McGill University Health Centre and the Department of Medicine, the [‖]Department of Pharmacology and Therapeutics, and the **Department of Biochemistry, McGill University, Montreal, Quebec H3G 1A4, Canada, the [§]Laboratory of Proteomics and Analytical Technologies, Advanced Technologies Program, SAIC-Frederick Inc., NCI-Frederick, National Institutes of Health, Frederick, Maryland 21702, and the [¶]Department of Physiology, Southern Illinois University, School of Medicine, Carbondale, Illinois 62901*

Background: The mechanism mediating hormone-induced steroidogenesis involves multiprotein complexes.
Results: 14-3-3γ is identified as a hormone-induced regulator of STAR function.
Conclusion: 14-3-3γ negatively regulates steroidogenesis by interacting with STAR, acting in a buffer capacity to sustain the STAR-mediated steroid formation for prolonged periods of time.
Significance: Characterizing the mechanisms regulating steroidogenesis contributes to our understanding of how steroids are synthesized.

Cholesterol is the sole precursor of steroid hormones in the body. The import of cholesterol to the inner mitochondrial membrane, the rate-limiting step in steroid biosynthesis, relies on the formation of a protein complex that assembles at the outer mitochondrial membrane called the transduceosome. The transduceosome contains several mitochondrial and cytosolic components, including the steroidogenic acute regulatory protein (STAR). Human chorionic gonadotropin (hCG) induces *de novo* synthesis of STAR, a process shown to parallel maximal steroid production. In the hCG-dependent steroidogenic MA-10 mouse Leydig cell line, the 14-3-3γ protein was identified in native mitochondrial complexes by mass spectrometry and immunoblotting, and its levels increased in response to hCG treatment. The 14-3-3 proteins bind and regulate the activity of many proteins, acting via target protein activation, modification and localization. In MA-10 cells, cAMP induces 14-3-3γ expression parallel to STAR expression. Silencing of 14-3-3γ expression potentiates hormone-induced steroidogenesis. Binding motifs of 14-3-3γ were identified in components of the transduceosome, including STAR. Immunoprecipitation studies demonstrate a hormone-dependent interaction between 14-3-3γ and STAR that coincides with reduced 14-3-3γ homodimerization. The binding site of 14-3-3γ on STAR was identified to be Ser-194 in the STAR-related sterol binding lipid transfer (START) domain, the site phosphorylated in response to hCG. Taken together, these results demonstrate that 14-3-3γ negatively regulates steroidogenesis by binding to Ser-194 of STAR, thus keeping STAR in an unfolded state, unable to induce maximal steroidogenesis. Over time 14-3-3γ homodimerizes and dissociates from STAR, allowing this protein to induce maximal mitochondrial steroid formation.

Steroidogenesis is the result of a series of enzymatic reactions mediating the metabolism of cholesterol to final steroid products in a tissue- and organelle-dependent manner (1). The rate-limiting step in steroidogenesis is the translocation of cholesterol from cytosolic sources to the inner mitochondrial membrane, where it is metabolized to pregnenolone by the cytochrome P450 side-chain cleavage enzyme (CYP11A1). In adrenal glands and gonads, steroid synthesis is induced by pituitary adrenocorticotropin and gonadotropin hormones, respectively. In Leydig cells of testis, the luteinizing hormone/chorionic gonadotropin (LH/CG) binds to the LH G-protein-coupled receptor), resulting in the rapid induction of the secondary messenger cAMP, which in turn increases protein phosphorylation, protein synthesis, and mobilization of cholesterol (2, 3). These actions ultimately result in the assembly of a protein complex called the transduceosome at the outer mitochondrial membrane (OMM),[4] through which import of cholesterol from the OMM to the inner mitochondrial membrane occurs (4–6). The trans-

* This work was supported by Canadian Institutes of Health Research Grant MOP102647 and a Canada Research Chair in Biochemical Pharmacology (to V. P.). The Research Institute of McGill University Health Centre was supported by a Center grant from Le Fonds de la Recherche du Québec-Santé.
[1] Supported in part by a predoctoral fellowship from the Research Institute of McGill University Health Centre.
[2] Supported in part by a postdoctoral fellowship from the Research Institute of McGill University Health Centre.
[3] To whom correspondence should be addressed: The Research Institute of the McGill University Health Center, 1650 Cedar Ave., C10-148, Montreal, Quebec H3G 1A4, Canada. Tel.: 514-934-1934 (ext. 44580); Fax: 514-934-8439; E-mail: vassilios.papadopoulos@mcgill.ca.

[4] The abbreviations used are: OMM, outer mitochondrial membrane; ACBD3, acyl-CoA binding domain-containing protein 3; BN, blue native; hCG, human chorionic gonadotropin; PKAIα, PKA regulatory subunit RIα; STAR, steroidogenic acute regulatory protein; START, STAR-related sterol-binding lipid transfer domain; TAT, trans-activator of transcription protein TSPO, translocator protein (18 kDa); VDAC, voltage-dependent anion channel; qPCR, quantitative PCR; Bis-Tris, 2-[bis(2-hydroxyethyl)amino]-2-(hydroxymethyl)propane-1,3-diol.

duceosome consists of several cytosolic and mitochondrial proteins, such as the translocator protein (18 kDa) TSPO, a high affinity cholesterol- and drug-binding protein that plays a major role in cholesterol import across the OMM (4). TSPO is enriched at the contact sites of the inner mitochondrial membrane and OMM along with another transduceosome protein, the voltage-dependent anion channel (VDAC). It has been demonstrated that several cytosolic proteins of the transduceosome, such as protein kinase A (PKA), acyl-CoA binding domain-containing protein 3 (ACBD3, also known as PAP7), and steroidogenic acute regulatory protein (STAR), assist in the import of cholesterol to the inner mitochondrial membrane (4, 6). High levels of cAMP activate the PKA regulatory subunit RIα (PKARIα), which is brought into the proximity of STAR through its association with ACBD3. PKA RIα is then able to phosphorylate STAR (4, 7, 8). STAR (STARD1) is a 37-kDa cytosolic protein that is expressed predominantly in gonads and adrenal glands (9) and plays a significant role in steroidogenesis (10–13). Upon hormonal stimulation, STAR levels increase rapidly (9) This protein contains a mitochondrial signal sequence (62 N-terminal amino acids) that confines its function to the OMM (14, 15). Phosphorylation of the Ser-194 residue of STAR increases its activity by 50%, resulting in maximal activity in steroid production (16–19). Import of STAR from the OMM results in the formation of the 30-kDa "mature" STAR, which terminates its function (14, 19–21). The STAR C terminus is a 210-amino acid hollow, hydrophobic, sterol binding domain called the STAR-related lipid transfer (START) domain through which STAR binds cholesterol with 3 μM affinity (10, 22–26). The presence of the START domain at the OMM is sufficient to promote cholesterol transfer, as overexpression of STAR in steroidogenic cells has been shown to increase pregnenolone formation in the absence of hormonal stimulation (27). In steroidogenic cells, STAR expression is tightly regulated (15, 28). Reduction or deletion of the *Star* gene or knockdown of the STAR protein arrests steroidogenesis (27, 29, 30). Mutations of STAR lead to the development of congenital lipoid adrenal hyperplasia, a condition in which cholesterol accumulates in adrenal or gonadal cells (1, 29).

To further understand the changes occurring in steroidogenic cell mitochondria in response to hormone treatment, we analyzed native mitochondrial protein complexes from control and hormone-treated MA-10 cells using mass spectrometry and identified the presence of members of the 14-3-3 family of proteins. The 14-3-3 proteins are small (27–32 kDa) acidic proteins that are highly conserved across species (31–33). They act as scaffolds and chaperones (33–35) and regulate cell signaling, cell division, apoptosis, gene transcription, DNA replication, and cytoskeletal formation and integrity. In mammals, seven 14-3-3 isoforms exist (36, 37). All 14-3-3 isoforms contain an N-terminal dimerization domain through which they homo/heterodimerize. Depending on the combination of dimers formed, 14-3-3 proteins carry out distinct physiological functions (38, 39). The 14-3-3 C terminus is the target binding domain through which these proteins bind to more than 200 target proteins (40–42). Despite the high percentage of homology between 14-3-3 isoforms, their targets are isoform-specific (34). Based on our observation that 14-3-3γ is increased 4-fold upon hCG stimulation, we investigated the role of this protein in the regulation of steroidogenesis and identified protein targets mediating its action in this pathway. The results demonstrate that 14-3-3γ binds to STAR and acts as a negative regulator of steroid formation.

TABLE 1
Sequences used for siRNA

14-3-3γ	DsiRNA 1	5′-CGCUUGUACUGUUUGGAAAUGACCT-3′
		3′-GGGCGAACAUGACAAACCUUUACUGGA-5′
	DsiRNA 2	5′-ACACUCAAUUGUAGUUUACAGUATT-3′
		3′-AUUGUGAGUUAACAUCAAAUGUCAUAA-5′
	DsiRNA 3	5′-CCACUAGGAAGAGGCAGUUCACUTG-3′
		3′-UGGGUGAUCCUUCUCCGUCAAGUGAAC-5′

EXPERIMENTAL PROCEDURES

Cell Culture, Treatments, and Steroid Measurement—MA-10 mouse Leydig tumor cells (kindly provided by Dr. M. Ascoli, University of Iowa, Ames) were maintained in DMEM/nutrient mixture F-12 (Invitrogen) supplemented with 5% fetal bovine serum, 2.5% horse serum, and 1% penicillin and streptomycin at 37 °C and 3.7% CO_2. For the time-course experiments, cells were incubated with cell culture media without serum, supplemented with 1 mM 8-bromo-cAMP (Enzo Life Sciences) or 50 ng/ml hCG (kindly provided by Dr. A. F. Parlow, the National Hormone and Peptide Program, Harbor-UCLA Medical Center) as indicated. The time-course treatment was carried out for 15, 30, 60, and 120 min as indicated in the corresponding figures of each experiment. To inhibit gene transcription, 10 μg/ml actinomycin D (Sigma) was added in media without serum in the presence of 1 mM cAMP.

When the trans-activator of transcription protein (TAT) peptide was used, 1×10^3 MA-10 cells were cultured in Waymouth MB752/1 medium containing 15% horse serum for 24 h. The 250 nM TAT peptide treatments were performed for 90 min. For the 14-3-3γ knockdown studies, 4×10^5 MA-10 cells were plated in a gelatin-coated 100-mm cell culture dish and incubated for 24 h. 5, 10, 20, and 50 nM 14-3-3γ siRNA of a mixture of 3 predesigned siRNAs (Table 1, Integrated DNA Technologies) were tested. Hypoxanthine-guanine phosphoribosyltransferase siRNA was used at 10 nM as a positive control, and a scrambled negative control was purchased from the same provider. The optimal siRNA concentration of 20 nM was selected for both 14-3-3γ and scrambled siRNA. Cells were incubated for 72 h in a mixture of 25 μl of Lipofectamine RNAiMAX (Invitrogen), 2.5 ml of Opti-MEM transfection medium, and 2.5 ml of DMEM/F-12 media without antibiotic supplemented with serum as previously explained. Progesterone levels were measured by radioimmunoassay (RIA) in triplicate with beta counter LS5801 (Beckman). Protein levels in each well were measured by using 1 N NaOH extraction buffer and the Bradford dye assay (Bio-Rad) using a Beckman spectrophotometer.

Mass Spectrometry Analysis of Mitochondria—Mitochondria were isolated by differential centrifugation as previously described (6). Briefly, confluent MA-10 control cells were treated with 50 ng/ml hCG for 2 h, washed twice with PBS, harvested in buffer A (10 mM HEPES-KOH (pH 7.5), 0.2 M mannitol, 0.07 M sucrose, 1 mM EDTA, and 1× Complete Protease

Inhibitor Mixture Tablets (Roche Diagnostics)) using a cell lifter, and centrifuged at 500 × *g* for 10 min. The cell pellet was resuspended in 5 volumes of buffer A, incubated at 4 °C for 10 min, and then centrifuged at 500 × *g* for 10 min. The cell pellet was resuspended in 5 volumes of buffer B (40 mM HEPES-KOH (pH 7.5), 500 mM sucrose, 160 mM potassium acetate, and 10 mM magnesium acetate with 1× Complete Protease Inhibitor Mixture Tablets) and homogenized using an electric Potter-Elvehjem grinder (glass Teflon) for 10 passes. Cells were centrifuged at 500 × *g* for 10 min. The cell pellet was resuspended in 5 volumes of buffer B with a glass-glass homogenizer (20 passes) and centrifuged at 500 × *g* for 10 min. The supernatant was pooled and centrifuged at 10,000 × *g* for 10 min at 4 °C to form a mitochondrial pellet that was further resuspended in 1 ml of buffer B and centrifuged at 10,000 × *g* for 10 min to enrich mitochondrial purity. The mitochondria were resuspended in buffer B at a final concentration of 1 mg/ml. Blue native PAGE (BN-PAGE) was performed as described by Simpson, in which 50 μg of mitochondria, both control and treated, were pelleted and solubilized with 1% digitonin buffer (20 mM Tris-HCl, 0.1 mM EDTA, 50 mM NaCl, 10% (w/v) glycerol, 1% digitonin (Invitrogen), and 1 mM PMSF) for 20 min on ice. Mitochondria were then centrifuged at 10,000 × *g* for 10 min. BN-PAGE loading dye (5% (w/v) Coomassie Brilliant Blue G-250, 500 mM ϵ-amino-*n*-caproic acid, and 160 mM Bis-Tris (pH 7.0)) was added to the sample supernatants, loaded onto a 4–16% native gel (Invitrogen), and run at 34 V overnight. The native gel spots cut from control and hCG-treated mitochondria at 66 kDa were in-gel-digested and analyzed via mass spectrometry as previously described (6), or the BN-PAGE was further transferred to a PVDF membrane for detection of 14-3-3γ and -ϵ in native mitochondrial complexes using 1:1000 dilutions of specific antibodies (Santa Cruz Biotechnology). The membranes were stripped using 8 ml of Restore Plus Western blot Stripping Buffer (Thermo Scientific) and reblotted using a 1:1000 dilution of cytochrome *c* oxidase antibody (Abcam, Cambridge, UK).

Immunohistochemistry—Adult mouse testis sections (4–6 μm; Cytochem Inc., Montreal, QC) were fixed using 4% formaldehyde for 20 min at −20 °C. Cells were washed with 1× PBS for 5 min at room temperature and permeabilized with 10% Triton X-100 for 3 min. The sections were blocked with 10% goat serum in a 1% BSA solution for 1 h at room temperature. Cells were incubated overnight at 4 °C in a 1:50 dilution of 14-3-3γ antibody in a humidified chamber. The following day cells were washed with 1× PBS for 5 min at room temperature twice and stained with secondary anti-rabbit IgG $F(ab')_2$ fragment (Alexa Fluor 488 conjugate; Invitrogen) for 1 h at room temperature. Cells were washed, and a 1:250 dilution of Hoechst (Enzo Life Sciences) was used for nuclear staining for 30 min at room temperature. Sections were maintained in one drop of mounting media (Invitrogen), and an Olympus inverted microscope was used for imaging using 20× or 40× lenses.

Immunoblot Analysis—MA-10 cells (6×10^5 per well) were cultured in 6-well gelatin-coated plates in triplicate for 24 h. A cAMP time-course treatment was carried out. Cells were washed twice in 4 ml of 1× PBS and harvested. Proteins were extracted using radioimmune precipitation lysis buffer (Cell Signaling Technology) or m-Per buffer (Thermo Scientific) in transcription blocker experiments, and protein levels were measured. Proteins (10 μg) were solubilized in Laemmli loading buffer and heated at 65 °C for 5–10 min. Samples were loaded directly onto a 4–20% Tris-glycine polyacrylamide gel (Invitrogen). Separated proteins were electrotransferred onto PVDF membranes. Membranes were blocked using 10% milk and blotted with a 1:1000 dilution of 14-3-3γ-specific or STAR antibody (43) at 4 °C overnight. The following day the membranes were washed with 1× Tween-Tris-buffered saline twice at room temperature and incubated with secondary anti-rabbit IgG HRP-linked antibody (Cell Signaling Technology) for 1 h with shaking at room temperature to detect 14-3-3γ. Membranes were developed using ECL streptavidin horseradish peroxidase conjugate (GE Healthcare) and imaged with a Fujifilm LAS-4000. The membranes were further washed and stripped using 8 ml Restore Plus Western blot Stripping Buffer at 37 °C for 20 min, washed, blocked, and blotted with a 1:3000 dilution of anti-glyceraldehyde-3-phosphate dehydrogenase (GAPDH) antibody (Trevigen) overnight at 4 °C as a loading control. Relative expression of proteins was assessed by measuring the band intensity (AU) and background intensity (BG) for each lane and calculating (AU-BG)/mm^2.

TABLE 2
Quantitative PCR primers used
HPRT, hypoxanthine-guanine phosphoribosyltransferase.

14-3-3γ	Forward	CGGACAGAAGAAGATCGAGATGGTCCG
	Reverse	GTTGTCCAGCAGGCTCAGCA
STAR	Forward	ACCAGGAAGGCTGGAAGAAGGAAA
	Reverse	ACCAGGAAGGCTGGAAGAAGGAAA
HPRT	Forward	GCGTCGTGATTAGCGATGATGAAC
	Reverse	ACCGACTGGATGGCTGATGAATGA

Quantitative Real-time PCR Analysis—MA-10 cells (2×10^5 per well) were cultured in 12-well gelatin-coated plates in triplicate and incubated overnight to reach 90% confluency. Time-course treatment with cAMP was performed. Cells were washed with 1 ml 1× PBS and harvested. RNA was extracted using RNeasy Mini kit (Qiagen). The mRNA concentration was measured with a Nanodrop 1000 spectrophotometer (Thermo Scientific). Exactly 1 μg of total RNA was used for RT-PCR using random hexamer primers (Roche Diagnostics) according to the manufacturer's manual. Quantitative PCR (qPCR) was conducted using 2 μl of RT-PCR product with LightCycler 480 SYBR Green I Master Mix (Roche Diagnostics), and primers were purchased from Integrated DNA Technologies (Table 2). Hypoxanthine-guanine phosphoribosyltransferase primers were used as an endogenous control at the each time point of cAMP treatment. Quantitative PCR was performed in triplicate, and the ΔΔCt method was used to demonstrate the relative transcription of the target gene compared with the reference gene.

Immunocytochemistry and Confocal Microscopy—MA-10 cells (2×10^4 per well) were plated in 96-well glass-bottom dishes (Fluorodish, WPI, Sarasota, FL) in triplicate and incubated until 60% confluent. Time-course treatment with cAMP was performed. Cells were fixed with 4 °C methanol for 3–5 min, permeabilized with 10% Triton X-100 for 3 min, and blocked with 10% goat serum for 1 h at room temperature. Cells were incubated in a 1:25 dilution of 14-3-3γ antibody and 5

TABLE 3
TAT peptide sequences and proposed binding sites
CAH, congenital adrenal hyperplasia.

No.	TAT peptide	Motif	Amino acid	Site	M_r
					Da
I	YGRKKRRQRRRGMGQVRRRSSLLGSQL	14-3- Mode I	52–58	Cleavage site (37/32/30 kDa)	3286.88
II	YGRKKRRQRRRGPGVLRDFVSVRCTK	14-3- Mode II	181–187	Mutation leads to CAH	2950.5
III	YGRKKRRQRRRGCTKRRGSTCVLAG	14-3- Mode II	191–196	Phosphorylation increases STAR activity; mutation leads to CAH	3175.8

μg/ml cytochrome *c* oxidase antibody (Abcam) overnight at 4 °C. The next day the wells were washed with 1× PBS and stained with secondary anti-rabbit IgG $F(ab')_2$ fragment (Alexa Fluor 488 conjugate) and anti-mouse IgG $F(ab')_2$ fragment (Alexa Fluor 555 conjugate; Cell Signaling Technology) at room temperature for 1 h. Cells were washed with 0.5 M Tris-HCl (pH 7.6), and an appropriate concentration of DAPI was used for nuclear staining for 5 min at room temperature. Cells were maintained in ultra-pure water. Confocal microscopy was performed using an Olympus Fluoview FV1000 laser confocal microscope with a 100× lens. Images were imported into Corel Draw X5 software, and images of representative cells from each well were selected.

Cross-linking—MA-10 cells (1×10^6 per Petri dish) were plated in gelatin-coated 100-mm Petri cell culture dishes overnight to reach 90% confluency. Medium was replaced with Dulbecco's modified Eagle's limiting medium supplemented with 10% FBS and 105 mg/liter photo-leucine and 30 mg/liter photo-methionine (Thermo Scientific). Cells were incubated for 22 h followed by cAMP time-course treatment. Medium was decanted and replaced with 4 ml of 1× PBS. Cross-linking was performed immediately using a 3UV lamp (UVP) for 16 min at 365 nm at a distance of 1 cm from the surface of the Petri dishes.

Co-immunoprecipitation—Co-immunoprecipitation was performed using a Dynabeads co-immunoprecipitation kit (Invitrogen). The antibody coupling process was performed using 14-3-3γ antibody following the manufacturer's recommendations, yielding 10 mg/ml antibody-coupled beads. Cross-linked protein lysates of MA-10 cells were harvested according to the manufacturer's recommendations. Proteins were collected in extraction buffer A (containing 1× immunoprecipitation buffer, 1 M NaCl, and protease inhibitor tablets without EDTA) and 0.5 mg of protein was precipitated with 150 μl of 10 mg/ml antibody-coupled beads rotating at 4 °C for 1 h. When studying 14-3-3γ dimerization, 0.1 mg of the protein lysate was used for co-immunoprecipitation. The precipitated samples were loaded on 4–20% Tris-glycine gels. MA-10 protein (10 μg) was used in the native state before and after 2 h of cAMP treatment (indicated on the gels as *IB* and *NCL*) or in the cross-linked state before and after 2 h of cAMP treatment (indicated on the gels as *IB* and *CL*). The immunoblot analysis was carried out as previously described, and the following antibodies and dilutions were used to blot the membranes: anti-14-3-3γ and anti-14-3-3ζ (1:1000 dilutions, Santa Cruz Biotechnology), anti-TSPO (1:5000 dilution (8)), anti-STAR (1:2000 dilution), and anti-ACBD3 (1:1000 dilution (44)), anti-PKARIα (1:1000 dilution, Santa Cruz Biotechnology), and anti-VDAC1 (2 μg/ml, Abcam). Secondary antibodies were used at the dilution factors previously mentioned.

Duolink and Confocal Microscopy—MA-10 cells (1×10^3 per well) were cultured in a 96-well glass-bottom dish (Fluorodish, World Precision Instruments) in triplicate and incubated overnight. Cells were treated in a time-course with cAMP as previously discussed. Cells were fixed using 3.7% formaldehyde for 15 min in 37 °C, washed with 1× PBS twice at room temperature, and permeabilized with 10% Triton X-100 for 1 min at room temperature. The Duolink II Red Starter Kit (Olink Bioscience) was used following the manufacturer's recommendations. Primary antibodies were used in combinations of 14-3-3γ (anti-mouse; Santa Cruz Biotechnology) and STAR (anti-rabbit) or 14-3-3γ (anti-mouse and anti-rabbit) overnight at 4 °C. Mitochondria and nuclei were stained using Mito-ID and Hoechst, respectively, both in 1:250 dilutions (Enzo Life Sciences) for 30 min at 37 °C. Cells were washed and maintained in ultra-pure water. An Olympus Fluoview FV1000 laser confocal microscope equipped with a 100× lens was used to detect protein-protein interactions between 14-3-3γ and either STAR or itself. Z stacks were captured from the bottom to the top of the cell nucleus. Images were imported into Corel Draw X5 software, and the images of representative cells from each well were selected.

Peptide Design and Labeling—Peptides were designed to contain an 11-mer of the HIV-1 TAT followed by a glycine residue and 15, 14, or 13 amino acids containing the 14-3-3 binding sites I, II and III, respectively, from the *Mus musculus* STAR protein (Table 3). Peptide I was synthesized by Bachem, and peptides II and III were synthesized by the Sheldon Biotechnology Center at McGill University, Quebec. Peptide labeling was carried out using the Oregon Green Labeling kit (Invitrogen), and the protein concentration and degree of labeling (mol of dye/mol of protein) were assessed by measuring absorbance at 280 and 496 nm using a Beckman spectrophotometer.

In Silico 14-3-3 Binding Motif Analysis—The presence of 14-3-3 binding motifs was assessed using uniprot motif scan to detect the 14-3-3 binding motif mode I (RS*X*pS*X*P, where R is arginine, S is serine, *X* is any amino acid, P is proline, and T is threonine), whereas mode II (R*XXX*pS*X*P) was detected manually (40, 42, 45).

Statistical Analysis—All experiments were performed in triplicate with three significant cell passages. RIA and qPCR have been performed in triplicate for each passage as well. The two-tailed unpaired *t* test was used for the immunoblot, and qPCR statistical analyses and a one-way ANOVA test was used for statistical analyses of the effect of the transcription inhibitor and protein-protein interaction studies.

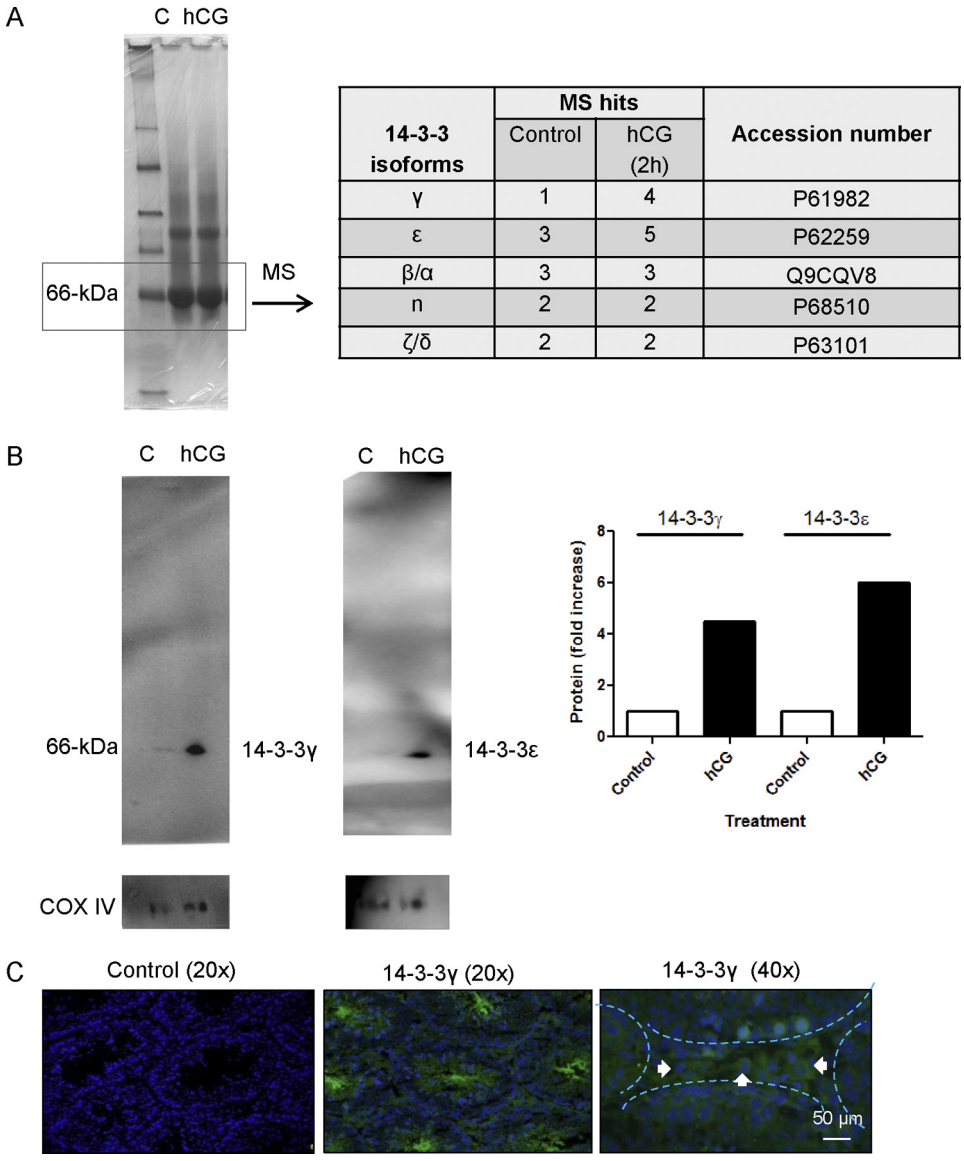

14-3-3 isoforms	MS hits		Accession number
	Control	hCG (2h)	
γ	1	4	P61982
ε	3	5	P62259
β/α	3	3	Q9CQV8
η	2	2	P68510
ζ/δ	2	2	P63101

FIGURE 1. **Presence of 14-3-3γ in native complexes of MA-10 cell mitochondria and testis of adult mouse.** *A*, BN-PAGE of native mitochondrial complexes from control and hCG-treated cells is shown. Mass spectrometry analysis indicated the presence of the 14-3-3 family of proteins in the mitochondrial 66-kDa complexes. The presence of the proteins in control *versus* hCG-treated cells is shown as mass spectrometry (MS) hits in the second and third column. *B*, BN-PAGE followed by dry transferring to PVDF membranes indicates the presence of 14-3-3γ and -ϵ in MA-10 cell mitochondria before and after hCG stimulation for 2 h. Relative expression of 14-3-3γ compared with the mitochondrial protein control cytochrome *c* oxidase (*COXIV*) is shown in the *bar graph*. *C*, immunohistochemistry of adult mouse testis sections shows the expression of 14-3-3γ in interstitial cells.

RESULTS

Mass Spectrometry Identifies Presence of 14-3-3 Proteins in MA-10 Mitochondria—To identify proteins that may play a role in cholesterol import, mitochondria were isolated from control or hCG-treated (for 2 h) MA-10 cells. The mitochondrial protein complexes were separated by BN-PAGE, and the major 66-kDa protein complex was analyzed using mass spectrometry (Fig. 1*A*). The results indicated the presence of members of the 14-3-3 protein family (γ, ϵ, β, η, and ζ) in the 66-kDa protein complex. However, only 14-3-3γ and -ϵ levels were increased after hCG treatment of the cells (4- and 1.6-fold, respectively). The presence and hormonal regulation of both isoforms at the mitochondria were further confirmed by immunoblot analysis of the BN-PAGE-separated proteins (Fig. 1*B*). The 4-fold induction by hCG of 14-3-3γ levels in mitochondria estimated by the number of MS hits was confirmed by BN-PAGE immunoblot analysis. However, a large >6-fold induction of 14-3-3ϵ levels was seen by BN-PAGE immunoblot analysis in hCG-treated mitochondria, in contrast to 1.6-fold increase in the number of MS hits found for the protein. This discrepancy may be due to the fact that proteins in BN-PAGE retain their native folding, and thus, hCG treatment may have allowed for better exposure of the 14-3-3ϵ immunoreactive epitopes. Immunohistochemistry of adult mouse testis sections confirmed the presence of 14-3-3γ in interstitial Leydig cells of the testes (Fig. 1*C*).

Expression of 14-3-3γ in MA-10 Cells—To characterize the 14-3-3γ expression pattern and localization in MA-10 cells, we stimulated the cells with cAMP in a time-course of up to 2 h. Immunoblot analysis demonstrated that the levels of 14-3-3γ

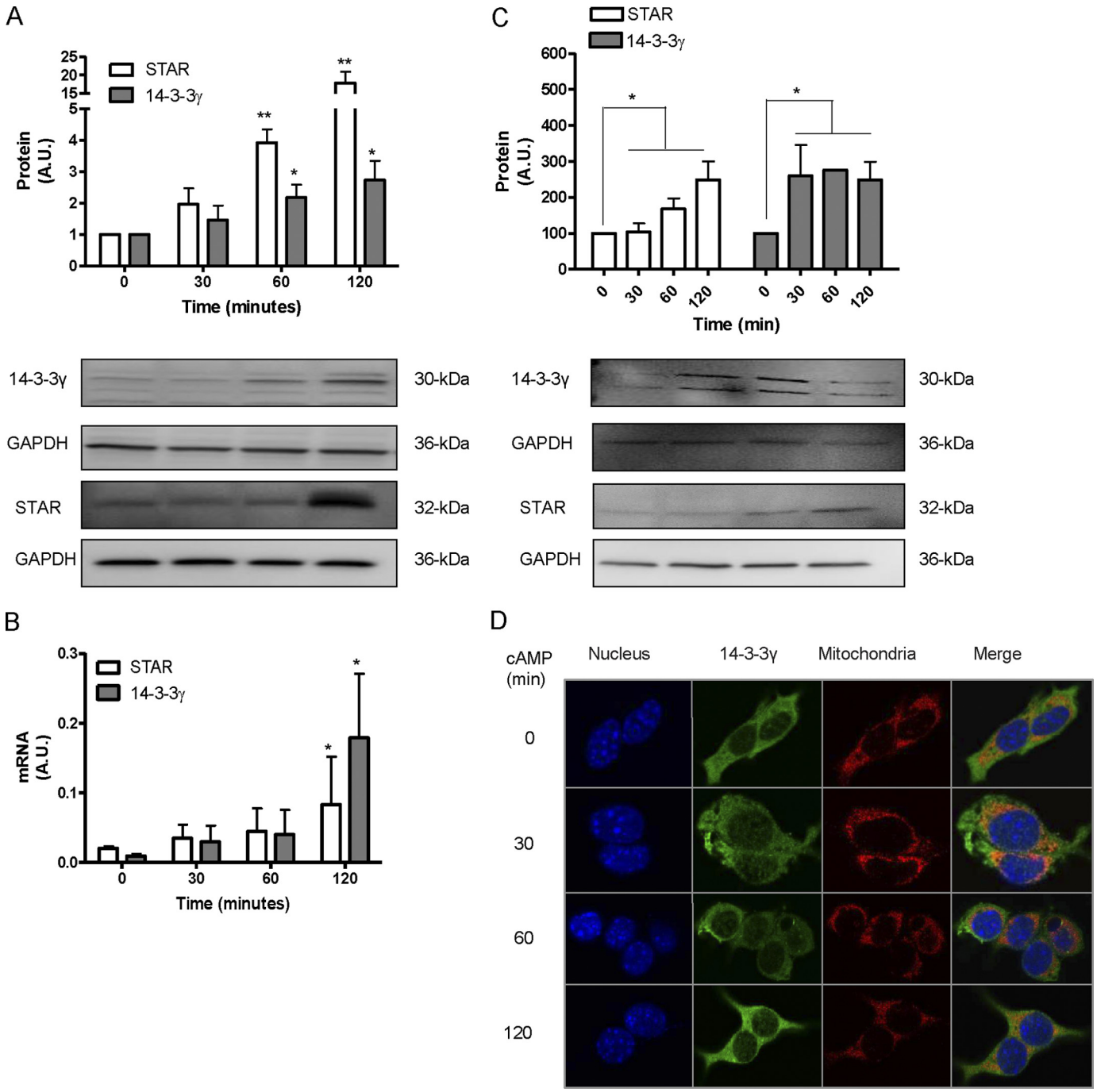

FIGURE 2. **The transcription and expression pattern of 14-3-3γ is similar to that of STAR.** MA-10 cells were stimulated with 1 mM cAMP in a time-course with the indicated time points. *A*, protein levels of STAR (*white bars*) and 14-3-3γ (*gray bars*) were assessed by immunoblot analysis. Representative immunoblots from three independent experiments show 14-3-3γ, STAR, and control GAPDH protein levels at 0, 30, 60, and 120 min after cAMP treatment. *A.U.*, absorbance units. *B*, levels of mRNA of both STAR (*white bars*) and 14-3-3γ (*gray bars*) were assessed by qPCR in triplicate. GAPDH mRNA levels were used for normalization. Results shown are the means ± S.D. from three independent experiments performed in triplicates. *C*, MA-10 cells were treated with the transcription inhibitor actinomycin D (10 μg/ml) and cAMP (1 mM). At the indicated time points cells were collected, and the expression levels of 14-3-3γ, STAR, and the control GAPDH were assessed by immunoblot analysis. Representative immunoblots from three independent experiments show 14-3-3γ, STAR, and control GAPDH protein levels at 0, 30, 60, and 120 min after cAMP treatment. *D*, localization of 14-3-3γ in MA-10 cells by immunocytochemistry is shown. DAPI, Alexa Fluor 488, and Alexa Fluor 555 were used to indicate nuclei, 14-3-3γ, and mitochondrial cytochrome *c* oxidase, respectively. The merge channel indicates that 14-3-3γ partially colocalizes with mitochondria.

increased after 1 h of cAMP treatment (Fig. 2*A*) or hCG (data not shown). This pattern was similar to that of STAR, a protein that is known to be rapidly induced in response to hormonal treatment (Fig. 2*A*). We then measured by qPCR the levels of mRNA for both STAR and 14-3-3γ with the same time-course treatment. The results indicated that mRNA levels of both proteins are induced only after 120 min of treatment (Fig. 2*B*), implying that the increase in protein levels of 14-3-3γ and STAR at earlier time points are likely due to the presence of pre-existing mRNA. To test this hypothesis we incubated the cells for different time periods in the presence of the transcription inhibitor actinomycin D to block new mRNA synthesis in

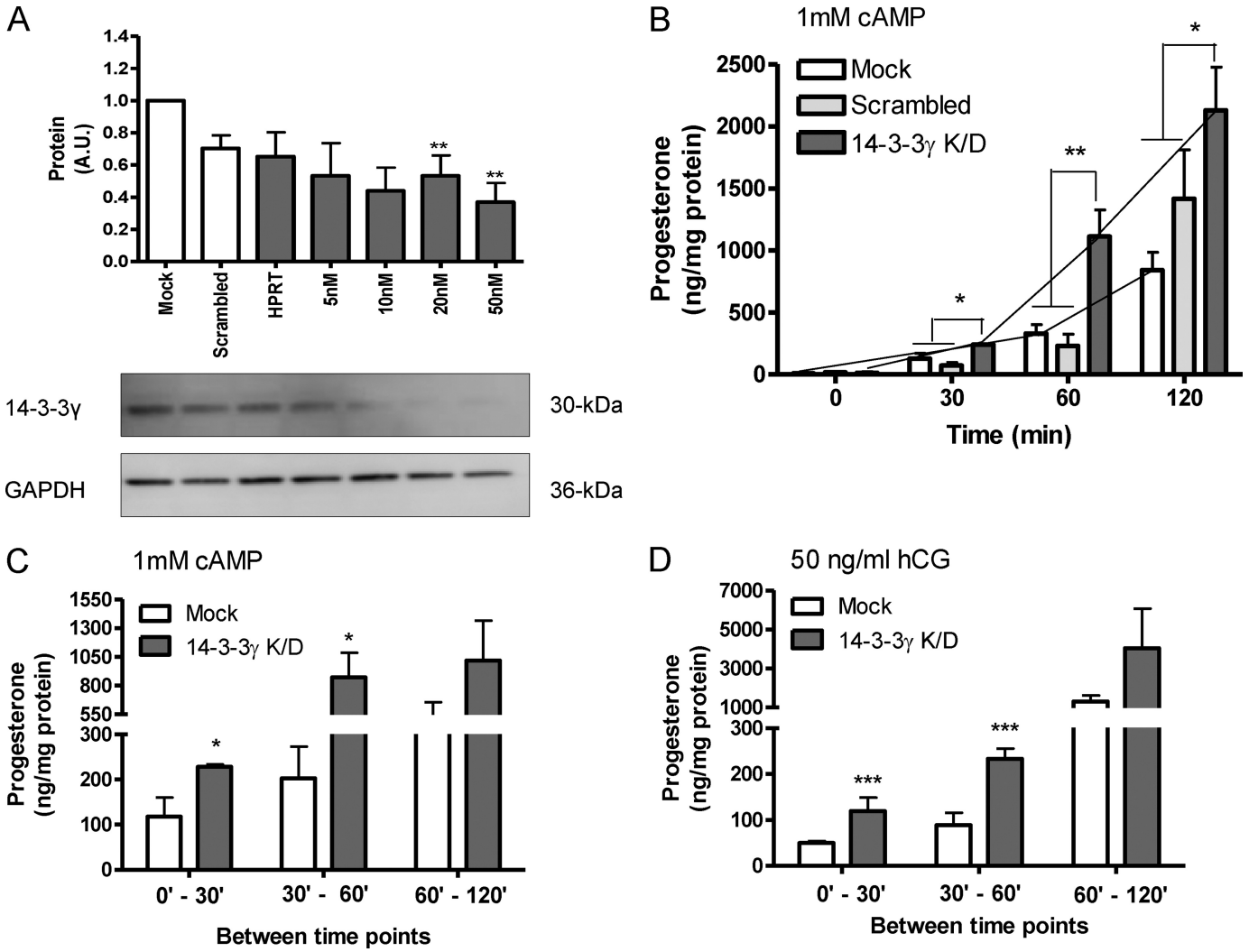

FIGURE 3. **Role of 14-3-3γ in steroidogenesis.** *A*, MA-10 cells were treated with different concentrations of 14-3-3γ isoform-specific siRNA and analyzed by immunoblot analysis. A representative immunoblot from three independent experiments is shown. *A.U.*, absorbance units. *HPRT*, hypoxanthine-guanine phosphoribosyltransferase. *B*, time-course treatment of MA-10 cells with 1 mM cAMP followed by RIA to measure progesterone levels in control cells (*white bars*), cells transfected with 20 nM scrambled siRNA (*light gray bars*), and cells treated with 20 nM 14-3-3γ siRNA (*dark gray bars*) is shown. *C*, data obtained in *B* was further analyzed to assess the rate of progesterone synthesis between the indicated time points (0–30, 30–60, and 60–120 min). *D*, time-course treatment of MA-10 cells with 50 ng/ml hCG is shown. Data obtained was analyzed to assess the rate of progesterone synthesis between the indicated time points (0–30, 30–60, and 60–120 min). Results shown are means ± S.D. from at least three independent experiments performed in triplicate.

the presence of cAMP. Immunoblot analysis demonstrated the presence of pre-existing mRNA for both 14-3-3γ and STAR as, despite inhibiting gene transcription, the levels of both proteins were induced by cAMP (Fig. 2*C*). However, distinct cAMP-induced time-dependent patterns of 14-3-3γ and STAR protein expression were seen (Fig. 2*C*). To characterize the localization pattern of 14-3-3γ in MA-10 cells, we performed the same time-course treatment with cAMP and fixed the cells. Immunofluorescence analysis demonstrated that 14-3-3γ is present in MA-10 cells and partially colocalizes with mitochondria as shown by its colocalization with the mitochondrial protein cytochrome *c* oxidase (Fig. 2*D*).

Decrease in 14-3-3γ Expression Increases Steroidogenesis—To investigate the role of 14-3-3γ in steroidogenesis, we assessed the ability of the cells to form steroids after siRNA knockdown of 14-3-3γ. After 72 h of treatment with 20 nM 14-3-3γ-specific siRNA, immunoblot analysis of the cell lysates showed a 55% reduction in 14-3-3γ protein levels (Fig. 3*A*). The MA-10 cells with reduced levels of 14-3-3γ were then treated with saturating concentrations of hCG or cAMP, and progesterone levels were measured by RIA. The results indicate that the decrease in 14-3-3γ protein levels results in increased steroid production (Fig. 3*B*). This effect was specific to 14-3-3γ siRNA used and could not be reproduced by scrambled siRNA (Fig. 3*B*). When these data were analyzed by calculating the increase in progesterone production between two consequent time points as shown in Fig. 3*C*, it became clear that the rate of progesterone synthesis significantly increased between 0 and 30 and between 30–60 min but not between 60 and 120 min of cAMP simulation. Thus, the significant increase seen after 120 min in Fig. 3*B* represents progesterone accumulation rather than increased rates of progesterone synthesis, as is the case for the earlier time periods. Similar results were obtained with hCG treatment (Fig. 3*D*). These experiments suggested a time-dependent negative regulatory role for this protein in MA-10 cells.

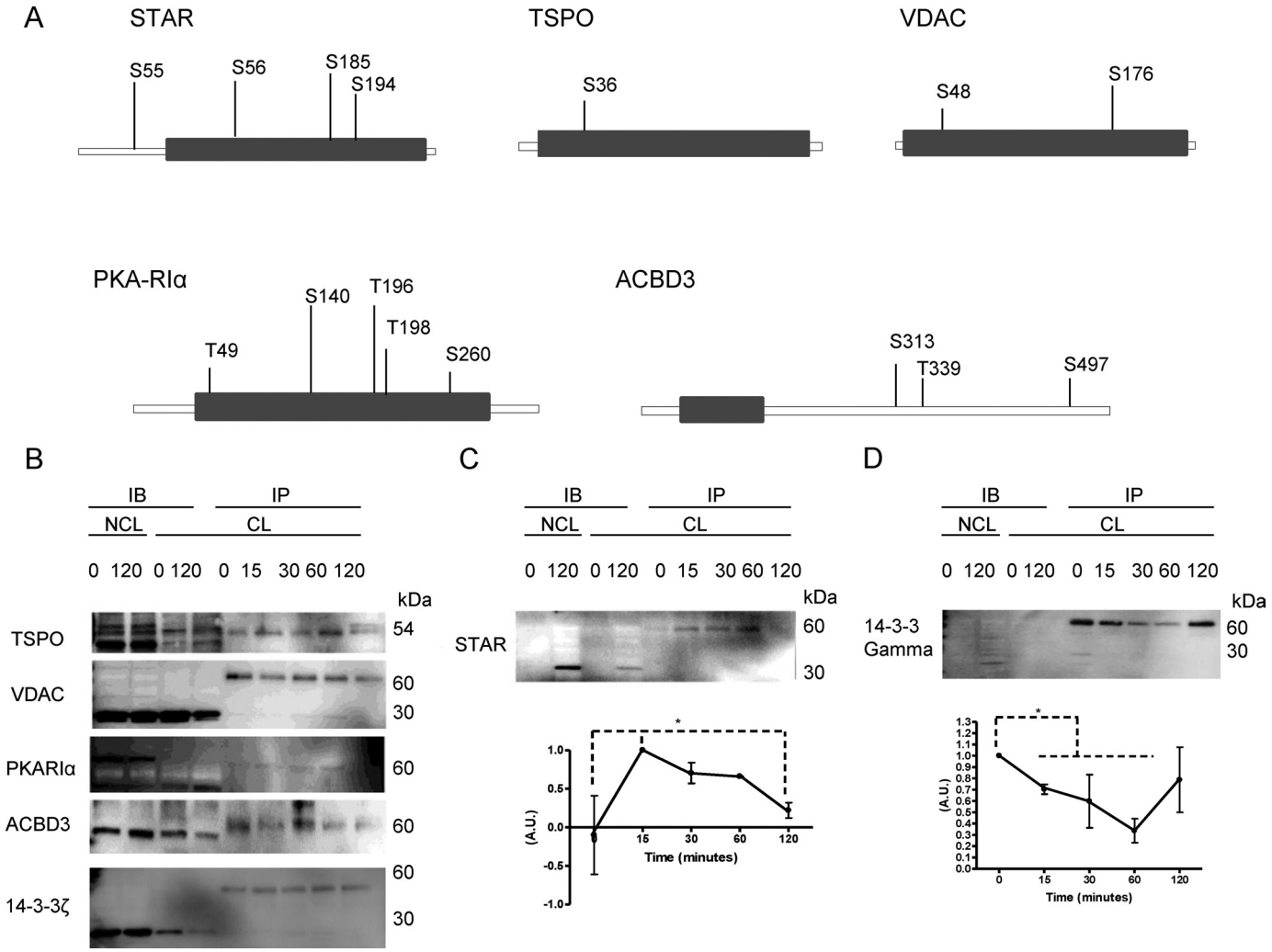

FIGURE 4. ***In silico* and *in vitro* identification of 14-3-3 target proteins in the transduceosome complex.** *A*, *in silico* analysis shows the presence of suboptimal 14-3-3 binding motifs of mode I and II in STAR, VDAC, PKARIα, and ABCD3. *B*, MA-10 cells were treated with 1 mM cAMP. Cross-linking was performed using photoactivatable amino acids in cell culture media and exposure to UV light after cAMP stimulation as indicated under "Experimental Procedures." Approximately 0.5 mg protein was co-immunoprecipitated (*IP*) with 14-3-3γ antibody followed by immunoblot analysis (*IB*) using antibodies for TSPO, VDAC, ABCD3, PKARIα, and 14-3-3ζ. *C*. Treatments were performed as described above (*B*), and STAR antibody was used to study binding between STAR and 14-3-3γ. *D*, treatments were performed as described above (*B*), and the homodimerization pattern of 14-3-3γ was studied by using the same antibody for both co-immunoprecipitation of 0.1 mg of protein and immunoblot. In *C* and *D* relative expression of proteins was analyzed as described under "Experimental Procedures." All results shown are representative of at least three independent experiments. *A.U.*, absorbance units. Cross-linked samples are indicated as *CL* and not cross-linked as *NCL*.

Identification of 14-3-3γ Target Proteins by Co-immuno precipitation—The majority of 14-3-3 target proteins contain 14-3-3 binding motifs present in three subtypes: modes I, II, and III (optimal motifs) and/or variations of these three modes (suboptimal motifs). We performed an *in silico* analysis to screen for the presence of 14-3-3 binding motifs on proteins known to play a role in steroidogenesis and identified mainly motifs of suboptimal modes I and II. One or more of these binding sites were found within STAR, TSPO, ABCD3, PKARIα, and VDAC (Fig. 4*A*). Because this analysis is not isoform-specific, further identification of 14-3-3γ-specific targets was performed by co-immunoprecipitation using 14-3-3γ antisera followed by immunoblot analysis with the indicated antibodies.

Considering the transience of the interaction between 14-3-3 proteins and their targets and the presence of suboptimal motifs on the transduceosome components, photo-activatable amino acids were used to cross-link 14-3-3γ and its target proteins by UV irradiation after stimulation of MA-10 cells with cAMP at the indicated time points. The results showed that 14-3-3γ binds to TSPO, VDAC, PKARIα, ACBD3, and 14-3-3ζ without cAMP or time dependence (Fig. 4*B*), whereas 14-3-3γ association/dissociation with STAR (Fig. 4*B*) and its homodimerization pattern (Fig. 4*C*) are time-dependent after cAMP treatment with inverse binding properties. In the absence of cAMP treatment, 14-3-3γ homodimers are present, and there is no detectable interaction with STAR. Upon 15 min of cAMP stimulation, 14-3-3γ homodimer levels are reduced, and its association with STAR is observed. The pattern of reduced levels of homodimerization and higher levels of STAR association is maintained up to 60 min of cAMP stimulation. At 120 min, the binding of STAR to 14-3-3γ is significantly reduced, whereas 14-3-3γ homodimer levels are increased compared with previous time points (Fig. 4, *C* and *D*).

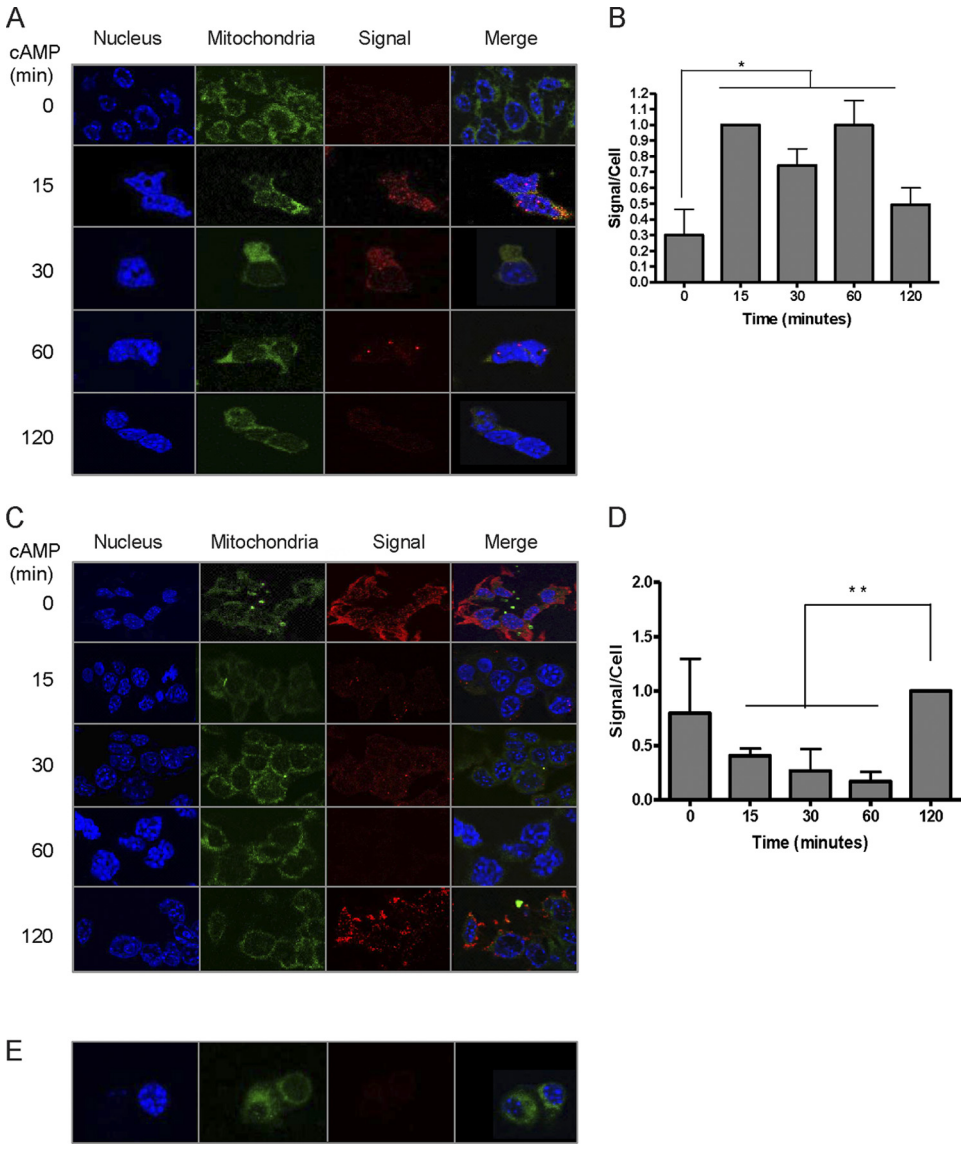

FIGURE 5. **Confirmation of STAR-14-3-3γ interactions using Duolink technology.** *A*, MA-10 cells were treated with 1 mM cAMP in a time-course as indicated. Duolink technology was performed using rabbit anti-STAR antibody and mouse anti-14-3-3γ antibody followed by the addition of proximity ligation assay probes. The red fluorescent tag was used to detect 14-3-3γ-STAR interactions, Hoechst for nuclei staining, and Mito-ID for mitochondrial staining. *B*, the signal per cell ratio was assessed for each time point using Olink software and normalized to the time point with the maximum interaction (15 min). *C* and *D*, a similar experiment was performed using two 14-3-3γ antibodies, raised in mouse and rabbit. The signal per cell ratio was measured and compared with that of the time point with the highest ratio (120 min). *E*, the experiment was performed as before, only in the absence of primary antibody to indicate background staining. Results shown are representative of at least three independent experiments.

Identification of 14-3-3γ Target Proteins by In-cell Immunoprecipitation—To confirm the pattern of 14-3-3γ-STAR interaction and compare it to that of 14-3-3γ homodimerization, we performed in-cell immunoprecipitation using Duolink technology followed by confocal microscopy. In this technique, interactions between the proteins of interest are shown as red fluorescent signals due to secondary antibody-linked oligonucleotide ligation and amplification, indicative of the interaction between the proteins recognized by the primary antisera. By comparing the intensity of signals at different time points after hormone treatment using Olink imaging software, the 14-3-3γ-STAR interaction and 14-3-3γ homodimerization were observed. Homodimerization of 14-3-3γ was seen at 0 and 120 min (Fig. 5, *A* and *C*). The results confirm the previous co-immunoprecipitation data (Fig. 4*C*) and demonstrate that the 14-3-3γ-STAR association is a time-dependent event showing an inverse pattern to that of 14-3-3γ homodimerization. Fig. 5*E* shows the negative control without primary antibody.

Identification of 14-3-3γ Site(s) of Interaction with STAR—We previously identified (Fig. 4*A*) *in silico* 14-3-3 binding motifs of mode I (amino acids 52–58) and of mode II (amino acids 181–187 and 191–196) on STAR (Fig. 6*A*). To assess the functionality of these 14-3-3 binding sites on STAR, these sequences were conjugated to an 11-mer TAT peptide (Fig. 6*B*; Table 3), a part of the HIV transcription factor TAT that can easily penetrate cell membranes and, therefore, acts as a shuttle for the conjugated sequence. Oregon Green-labeled peptides were found to be rapidly (within 15 min of treatment) transduced into the cells (Fig. 6*B*). Cells were treated for 15 min with cAMP to yield maximal STAR-14-3-3γ interaction (as shown in Figs. 4*C* and 5, *A* and *B*).

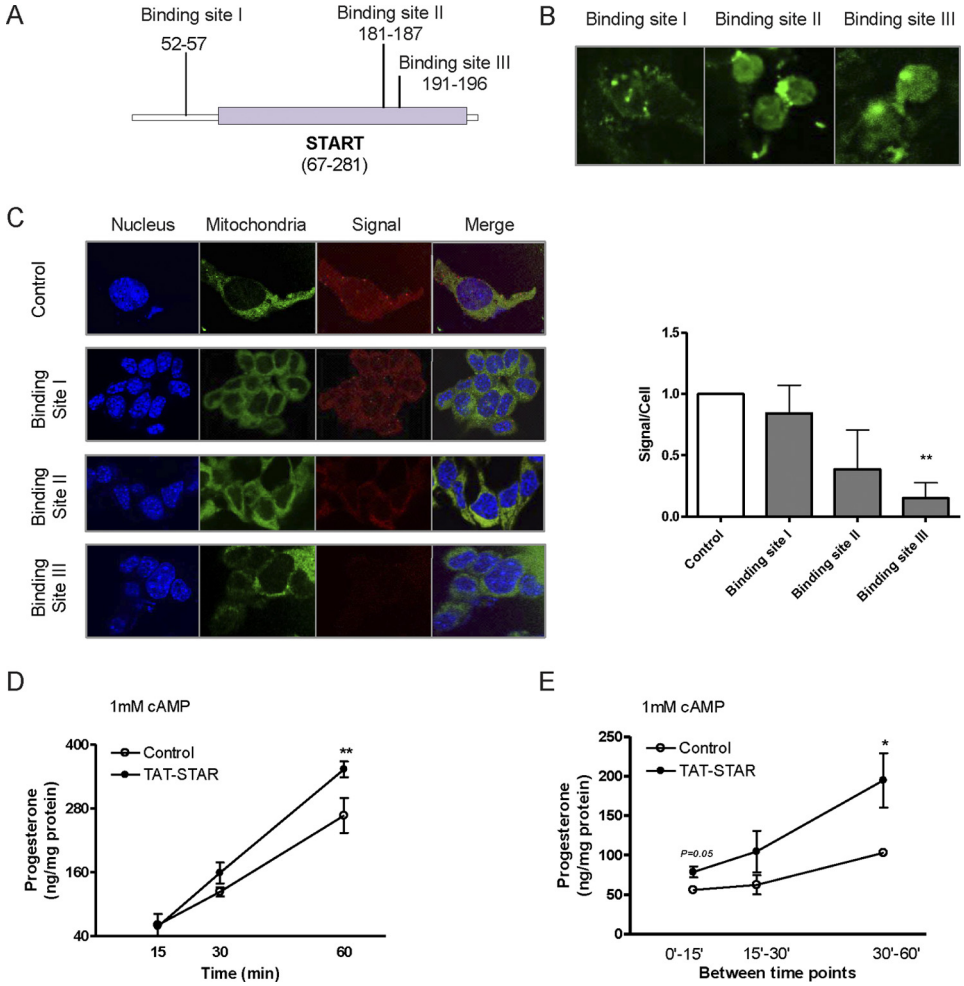

FIGURE 6. **Identification of the 14-3-3γ binding site on STAR.** *A*, the 14-3-3 binding motif mode I (residues 52–57) and mode II (residues 181–187 and 191–196) were detected *in silico* on STAR. Peptides containing a TAT peptide sequence followed by each of the 14-3-3 motifs on STAR were synthesized (Table 3). *B*, peptide labeling using Oregon Green 488 shows that TAT peptide sequences easily penetrate the MA-10 cell membrane and enter the cytoplasm, therefore acting as a shuttle for the 14-3-3 binding motifs on STAR. *C*, MA-10 cells were treated with 1 mM cAMP for 15 min to induce maximal STAR-14-3-3γ interactions. The *top panel* shows the control cells. In the second, third, and fourth panel, cells were treated for 90 min with 250 nM concentrations of the first, second, and third peptides, respectively, followed by 15 min of cAMP treatment. Duolink was performed using mouse anti-14-3-3γ antibody and rabbit anti-STAR antibody. The signal per cell was measured and normalized to the control, indicating that only peptide three significantly competes with STAR interaction with 14-3-3γ and blocks this interaction. *D*, levels of progesterone were measured in MA-10 cells treated with 250 nM of the STAR-competing peptides. Cells were treated with cAMP for 15–60 min to induce STAR-14-3-3γ binding, and progesterone levels were measured. *E*, data obtained in *D* were analyzed to assess the rate of progesterone synthesis between the indicated time points (0–15, 15–30, and 30–60 min). Results shown are the means ± S.D. from at least three independent experiments performed in triplicate. *Binding site I*, *II*, and *III* indicate the corresponding peptide I, II, and III used.

The interaction between 14-3-3γ and STAR was assessed using Duolink technology and confocal microscopy (Fig. 6*C*). These results indicated that the peptide containing the first 14-3-3 binding motif (mode I, amino acids 52–58) on STAR does not compete with STAR protein for interaction. The peptide containing the second 14-3-3 binding motif (mode II, amino acid 181–187), despite partial competition with STAR, did not significantly block the interaction between STAR and 14-3-3γ. However, the third peptide (mode II, amino acids 191–196) significantly competed with STAR and blocked the STAR-14-3-3γ interaction by 80% (Fig. 6*C*). MA-10 cells were then incubated with media containing 250 nM of the STAR-competing peptide followed by cAMP treatment for 15, 30, and 60 min, which are the time points during which STAR and 14-3-3γ interact (Fig. 4*C* and 5, *A* and *B*), and progesterone formation was measured. The results indicated that the negative regulatory role of 14-3-3γ is carried out through its interaction with STAR. When this interaction is inhibited due to the presence of a STAR-competing peptide, MA-10 cells produce higher levels of progesterone (Fig. 6*D*). Calculation of absolute values of progesterone formation between each two consequent time points showed an increasing rate of progesterone synthesis that reaches significantly higher levels between 30 and 60 min after cAMP treatment (Fig. 6*E*).

DISCUSSION

Hormonal induction of cholesterol import into mitochondria and thus steroidogenesis are mediated by the multiprotein complex known as the transduceosome. This complex is composed of mitochondrial and cytosolic proteins that contribute to the import of cholesterol into mitochondria, the rate-limiting step in steroid biosynthesis in the adrenal glands and gonads (1, 3, 4, 46). The transduceosome is formed of the OMM proteins TSPO and VDAC and the cytosolic proteins PKARIα,

ACBD3 (a member of the protein kinase A-anchoring proteins), and the hormone-induced and -activated STAR (4, 47, 48). The function of the transduceosome is to mediate and amplify the cAMP signal (48) at the cytosol/mitochondrion interface. Indeed, STAR functions at the OMM, and phosphorylation of this protein has been shown to be essential for its role in cholesterol mobilization across the OMM. Two PKA consensus sequences have been identified on STAR at Ser-55 and Ser-194 (7). Phosphorylation of the first serine residue is linked to the cleavage of the mitochondrial signal sequence of STAR, whereas phosphorylation of the second serine residue is responsible for maximal activity of the protein, which is required for steroidogenesis (16, 24). Therefore, STAR levels are tightly regulated in steroidogenic cells, and understanding the mechanisms underlying its regulation would provide insights into transduceosome protein-protein interactions and the regulation of steroidogenesis.

To find possible candidates that contribute to the regulation of steroidogenesis, native mitochondrial complexes of control and hormone-treated MA-10 Leydig cells were analyzed using mass spectrometry, which revealed the presence of members of the 14-3-3 family of proteins. A 4-fold induction in 14-3-3γ levels was observed upon hCG stimulation. The 14-3-3γ protein is known for its roles in regulating intracellular protein localization (49), the cell cycle, cell division, apoptosis (50), and mitogenic signaling (51) as well as its involvement in diseases such as Parkinson disease (52) and cancer (53). This protein has recently been identified as an oncogene (53, 54). Considering that MA-10 cells are a mouse Leydig cell line, we investigated and demonstrated the presence of 14-3-3γ in interstitial Leydig cells of the adult mouse testis. Based on the mass spectrometry results, the observation that 14-3-3 proteins associate with mitochondria, and the increase in 14-3-3γ levels upon cAMP treatment, we investigated whether 14-3-3γ plays a regulatory role in steroidogenesis.

Our studies demonstrate that 14-3-3γ is widely distributed within MA-10 cells and partially co-localizes with mitochondria. The transcription/translation pattern of 14-3-3γ is similar to that of STAR; both proteins are encoded by pre-existing mRNAs that are acutely translated upon cAMP stimulation. Interestingly, translation of pre-existing *Star* mRNA was induced by cAMP in a time-dependent manner with protein synthesis increasing over time and beyond 2 h upon cAMP treatment. However, the cAMP-induced translation of pre-existing *14-3-3γ* mRNA rapidly reached maximal levels at 30 min, suggesting that the mechanisms mediating the cAMP-induced translation of these two pre-existing mRNAs are distinct.

To understand the physiological role of 14-3-3γ in steroidogenic Leydig cells, we measured and compared steroid formation when 14-3-3γ levels were reduced after siRNA treatment. Progesterone formation in MA-10 cells was increased when 14-3-3γ levels were reduced, suggesting a negative regulatory role for this protein in steroidogenesis. Knockdown of 14-3-3γ led to a shift in the time frame of steroid production, as progesterone levels produced at each time point in the presence of 14-3-3γ was comparable with that of an earlier time point in the absence of 14-3-3γ. Further analysis of the data showed that 14-3-3γ acts during distinct periods of time after cAMP treatment, indicating a transient effect.

It has been previously shown that 14-3-3 proteins act as scaffolds through protein-protein interactions, inhibit protein modifications, alter the intrinsic activity of their target proteins, and alter the subcellular localization of their target proteins (33, 55). Through *in silico* and *in vitro* protein-protein interaction analysis, we identified STAR, TSPO, ACBD3, PKARIα, and VDAC as targets of 14-3-3γ. Therefore, we introduce 14-3-3γ as a new member of the transduceosome multiprotein complex. Based on the adaptor characteristics of this protein, it is possible that 14-3-3γ plays a role in the assembly of the transduceosome complex. *In vitro* and in-cell co-immunoprecipitation experiments revealed that 14-3-3γ does not interact with STAR in control MA-10 cells. However, hormonal treatment of the cells triggers the association of 14-3-3γ monomers with STAR for 15–60 min after treatment, a period when 14-3-3γ may play a negative regulatory activity on steroidogenesis.

Previous studies indicated that, although STAR levels are induced as early as 60 min upon hormonal stimulation, steroid formation reaches maximal levels no earlier than 2 h after stimulation (2, 56). The results presented herein suggest that this delay is based on the association of STAR with 14-3-3γ, leading to inhibition of STAR activity before 2 h post-stimulation. Because most likely not the entire STAR formed associates with 14-3-3γ, the available free STAR would exert some steroidogenic function without, however, reaching maximal activity. These results may also explain the reported lag between accumulation of the 37-kDa STAR and increase in pregnenolone production (1, 3, 4, 46). Dissociation of 14-3-3γ from STAR allows STAR to carry out its function at the maximal level, and therefore, high levels of steroids are produced under these conditions. Thus, 14-3-3γ seems to act in a buffer capacity to sustain the hormone- and cAMP-induced signal mediated by STAR for a longer period of time.

We further addressed the mechanism underlying 14-3-3γ dissociation from STAR after 2 h. Previous studies by Aitken *et al.* (34, 57, 58) showed that 14-3-3γ has a 95% tendency to form homodimers(33, 59). Our data suggest that 14-3-3γ dimerization occurs when the protein dissociates from STAR at 2 h after cAMP treatment. These studies suggest that 14-3-3γ is present as both homodimers and heterodimers with 14-3-3ζ, in control cells. Upon 15 min of cAMP stimulation, 14-3-3γ protein expression is increased, and homodimerization is reduced, whereas heterodimerization with 14-3-3ζ remains unaltered. Therefore, high levels of 14-3-3γ monomers are present, available to bind to STAR from 15 to 60 min post-treatment. At 120 min post-treatment, the high levels of cAMP-induced 14-3-3γ adopt a homodimeric conformation, likely displaying a dominant negative regulatory role, a well studied function of the 14-3-3 family of proteins (57–59). The structure, significant functional domains, and modification sites of STAR are well studied (10, 60). Therefore, identification of the site(s) of 14-3-3γ binding to STAR would provide insight into how the interaction between the two proteins occurs. We identified *in silico* the presence of three 14-3-3 binding motifs in three critical regions of STAR. These binding sites are placed at sites essential for (i) proteolytic cleavage from the 37-kDa form of the protein to the 32-kDa "intermediate, active" form and the 30-kDa "mature, inactive" form (1), (ii) activity (the site

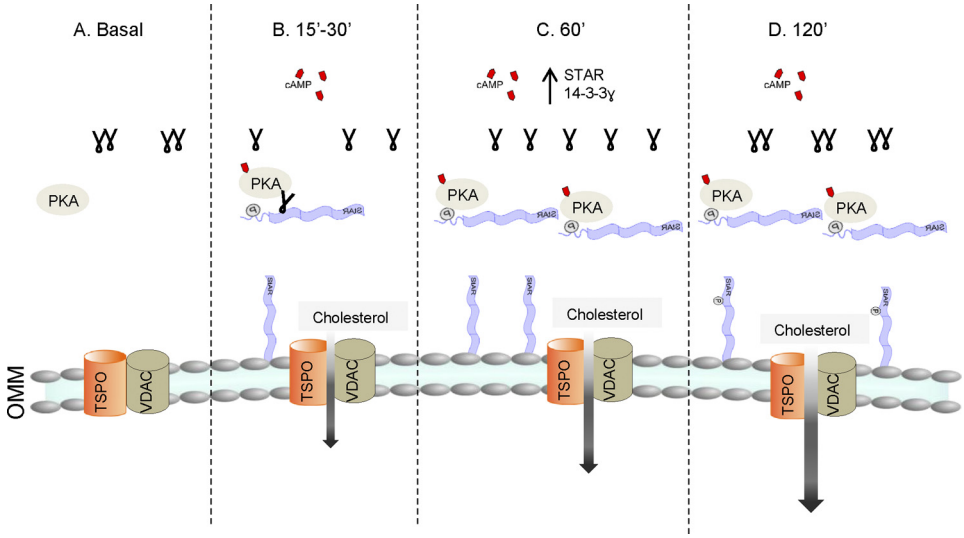

FIGURE 7. **Proposed model for the negative regulatory role of 14-3-3γ in steroidogenesis.** *A*, under basal conditions, 14-3-3γ is present in the form of homodimers. *B*, after 15 min of cAMP treatment, PKA gets activated, and 14-3-3γ homodimers dissociate, resulting in increased levels of 14-3-3γ monomers. 14-3-3γ monomers bind to STAR at residues 191–196 in the START domain and block the PKA consensus for Ser-194 phosphorylation. Thus, STAR is maintained at partial rather than maximal activity. *C*, at 60 min of cAMP treatment, the levels of both STAR and 14-3-3γ are increased significantly through translation of pre-existing mRNA. *D*, at 2 h of stimulation, 14-3-3γ levels are further increased leading to homodimerization, which likely carries out a dominant negative role for 14-3-3γ function. As a result, 14-3-3γ dissociates from STAR, allowing Ser-194 to be phosphorylated by PKARIα and further inducing STAR activity required for maximal steroidogenesis.

includes the Arg-182 residue, which if mutated leads to congenital adrenal hyperplasia) (16, 29, 29), and (iii) maximal activation (the site includes the Ser-194 residue, which is phosphorylated for maximal activity). These 14-3-3 binding motifs are of mode I and II. Several studies indicate that 14-3-3 protein targets contain optimal or suboptimal motifs as a result of adapting to their physiological requirement to transient binding and dissociation from 14-3-3 proteins (42, 45, 61). The majority of 14-3-3 targets, including STAR, contain suboptimal motifs (45, 57). To identify the specific 14-3-3γ binding site(s) on STAR, transducible peptides containing each of the three candidate 14-3-3-binding peptide sequences were used to assess the competition efficiency of each site with intact, endogenous STAR protein. The results indicate that, despite competition from at least two 14-3-3γ binding motifs with STAR, only one of the peptides significantly reduced STAR binding to 14-3-3γ. This motif is of mode II and contains the Ser-194 residue, which is essential for STAR phosphorylation and activation by PKA. Previous studies have suggested that the point mutation S194A reduces activity of STAR by 50% (16). It should be noted that 14-3-3γ-specific binding to the PKA consensus peptide sequence (R(R/K)*X*(S/T)) containing Ser-55 was not observed, suggesting that 14-3-3γ regulation of STAR activity is specific for the Ser-194 phosphorylation site rather than a general association with serine residues in a PKA consensus site. Treatment of MA-10 cells with the transducible peptide and further stimulation of these cells for 15–60 min with cAMP, the period of STAR-14-3-3γ interaction, showed an increase in steroid formation compared with control cells. This increase was triggered as early as 15 min and peaked after 60 min of stimulation, indicating that the specific role of 14-3-3γ in the negative regulation of steroidogenesis is through its association with and inhibition of STAR.

The specific 14-3-3 binding motif on STAR structure falls in a STAR region conserved across mammalian species (19, 62). Considering that the 14-3-3 family of proteins is highly conserved across species (63), we can speculate that the mechanism of STAR regulation by 14-3-3γ may also be conserved across species.

Based on immunoprecipitation and TAT peptide studies, the significant increase in steroid levels at 2 h after cAMP treatment may not be solely due to the induction in STAR levels but also to the release of STAR from 14-3-3γ, which allows it to be phosphorylated at Ser-194. Although cAMP-induced phosphorylation of newly synthesized STAR is critical for the induction of steroidogenesis, the 14-3-3γ-bound STAR would remain unphosphorylated and when released would provide additional pools of STAR to be phosphorylated, thus sustaining for a longer period of time the biological function of the protein. It is also important to note that this binding site is a part of the START domain (residues 76–281). Studies by Omura and co-workers (35) have shown that 14-3-3γ can identify and bind to unfolded mitochondrial proteins, helping them maintain this state. Indeed, in that report, 14-3-3γ was suggested to be a part of the mitochondrial import-stimulating factor (35, 64–66), which is a heterodimer of 14-3-3γ with 14-3-3ϵ (35). This area may prove to be interesting for investigating in the mechanism of protein import into mitochondria of steroidogenic cells.

Several studies since 1995 have dealt with the complexity of STAR structure. The START domain is conserved in mammals and plants, just like 14-3-3 proteins, and is shielded in the core of the STAR protein rather than exposed (60, 63). Therefore, few models were proposed to show the mechanism of binding and dissociation of cholesterol to the START domain. Miller and co-workers (26) have shown that, in acidic environments such as mitochondrial membranes, the 62-amino acid N terminus of STAR is more tightly folded than the START domain. They further proposed a molten globule model for STAR function that suggests that STAR is partially unfolded and has lost some of its tertiary structures while retaining its secondary

structure (array of α helices and β sheets). Therefore, cholesterol can access the START domain in the loosely folded C terminus (22, 26). The LeHoux (67) group also proposed a model showing that under neutral pH conditions and in the absence of cholesterol, a cavity is formed in the START domain. However, in the presence of cholesterol, this cavity is transformed to a "closed" conformation, and a reversible unfolding of the C-terminal helix of STAR takes place, providing access for the cholesterol molecule. Both of these models emphasize that STAR needs to be unfolded to allow for cholesterol binding. Therefore, because 14-3-3γ binds to the START domain, it might retain the unfolded structure, allowing cholesterol binding and subsequently altering STAR activity (22, 26, 68). Therefore, we suggest that 14-3-3γ dissociation from STAR is required for proper folding of the semi-folded STAR. However, we cannot rule out the possibility that 14-3-3γ can also act by binding and blocking STAR cleavage to the active form and/or binding to the site containing Arg-182, which if mutated leads to congenital adrenal hyperplasia.

Taken together, these results suggest a model for the negative regulatory role of 14-3-3γ in steroidogenesis (Fig. 7). This model proposes that after 15 min of hormonal stimulation, 14-3-3γ homodimers dissociate, allowing 14-3-3γ to interact with its target STAR. This 14-3-3γ-STAR interaction blocks the proper folding of STAR as the binding occurs at the START domain and blocks the Ser-194 PKA phosphorylation site. Lack of this phosphorylation prevents the induction of maximal STAR activity, leaving the protein with only partial activity. The association between 14-3-3γ and STAR is maintained up to 60 min post-stimulation, whereas the levels of both proteins are increased. However, the hormone-induced increase in 14-3-3γ expression further leads to dimerization of this protein, which manifests a dominant negative effect. This effect causes the dissociation of 14-3-3γ from STAR, leaving Ser-194 available for phosphorylation by PKA and enabling maximal activity. This system allows for the sustained production of steroids within 2 h of hormonal stimulation. In conclusion, although it is likely that 14-3-3γ may interact in Leydig cells with various proteins unrelated to the mechanism mediating the hormonal induction of steroid biosynthesis, the data presented herein demonstrate the determining role of 14-3-3γ in this process.

Acknowledgments—We thank Dr. Mario Ascoli (University of Iowa, Iowa City, IA) for supplying the MA-10 cell line, the National Hormone and Pituitary Program (NICHD, National Institutes of Health) for supplying the hCG, and Dr. Daniel B. Martinez-Arguelles for assistance in Duolink image analysis and computer illustrations.

REFERENCES

1. Stocco, D. M., and Clark, B. J. (1996) Regulation of the acute production of steroids in steroidogenic cells. *Endocr. Rev.* **17,** 221–244
2. Bakker, G. H., Hoogerbrugge, W., Rommerts, F. F., and van der Molen, H. J. (1983) LH-dependent steroid production and protein phosphorylation in culture of rat tumor Leydig cells. *Mol. Cell. Endocrinol.* **33,** 243–253
3. Pon, L. A., and Orme-Johnson, N. R. (1986) Acute stimulation of steroidogenesis in corpus luteum and adrenal cortex by peptide hormones. Rapid induction of a similar protein in both tissues. *J. Biol. Chem.* **261,** 6594–6599
4. Papadopoulos, V., Liu, J., and Culty, M. (2007) Is there a mitochondrial signaling complex facilitating cholesterol import? *Mol. Cell. Endocrinol.* **265,** 59–64
5. Rone, M. B., Fan, J., and Papadopoulos, V. (2009) Cholesterol transport in steroid biosynthesis. Role of protein-protein interactions and implications in disease states. *Biochim. Biophys. Acta* **1791,** 646–658
6. Rone, M. B., Liu, J., Blonder, J., Ye, X., Veenstra, T. D., Young, J. C., and Papadopoulos, V. (2009) Targeting and insertion of the cholesterol binding translocator protein into the outer mitochondrial membrane. *Biochemistry* **48,** 6909–6920
7. Hansson, V., Skålhegg, B. S., and Taskén, K. (1999) Cyclic-AMP-dependent protein kinase (PKA) in testicular cells. Cell-specific expression, differential regulation, and targeting of subunits of PKA. *J. Steroid Biochem. Mol. Biol.* **69,** 367–378
8. Li, H., Degenhardt, B., Tobin, D., Yao, Z. X., Tasken, K., and Papadopoulos, V. (2001) Identification, localization, and function in steroidogenesis of PAP7. A peripheral-type benzodiazepine receptor- and PKA (RIα)-associated protein. *Mol. Endocrinol.* **15,** 2211–2228
9. Clark, B. J., Wells, J., King, S. R., and Stocco, D. M. (1994) The purification, cloning, and expression of a novel luteinizing hormone-induced mitochondrial protein in MA-10 mouse Leydig tumor cells. Characterization of the steroidogenic acute regulatory protein (StAR). *J. Biol. Chem.* **269,** 28314–28322
10. Arakane, F., Kallen, C. B., Watari, H., Foster, J. A., Sepuri, N. B., Pain, D., Stayrook, S. E., Lewis, M., Gerton, G. L., and Strauss, J. F., 3rd (1998) The mechanism of action of steroidogenic acute regulatory protein (StAR). StAR acts on the outside of mitochondria to stimulate steroidogenesis. *J. Biol. Chem.* **273,** 16339–16345
11. Arakane, F., Kallen, C. B., Watari, H., Stayrook, S. E., Lewis, M., and Strauss, J. F., 3rd (1998) Steroidogenic acute regulatory protein (StAR) acts on the outside of mitochondria to stimulate steroidogenesis. *Endocr. Res.* **24,** 463–468
12. Kallen, C. B., Arakane, F., Christenson, L. K., Watari, H., Devoto, L., and Strauss, J. F., 3rd (1998) Unveiling the mechanism of action and regulation of the steroidogenic acute regulatory protein. *Mol. Cell. Endocrinol.* **145,** 39–45
13. Tuckey, R. C., Headlam, M. J., Bose, H. S., and Miller, W. L. (2002) Transfer of cholesterol between phospholipid vesicles mediated by the steroidogenic acute regulatory protein (StAR). *J. Biol. Chem.* **277,** 47123–47128
14. Epstein, L. F., and Orme-Johnson, N. R. (1991) Regulation of steroid hormone biosynthesis. Identification of precursors of a phosphoprotein targeted to the mitochondrion in stimulated rat adrenal cortex cells. *J. Biol. Chem.* **266,** 19739–19745
15. Stocco, D. M., and Sodeman, T. C. (1991) The 30-kDa mitochondrial proteins induced by hormone stimulation in MA-10 mouse Leydig tumor cells are processed from larger precursors. *J. Biol. Chem.* **266,** 19731–19738
16. Arakane, F., King, S. R., Du, Y., Kallen, C. B., Walsh, L. P., Watari, H., Stocco, D. M., and Strauss, J. F., 3rd (1997) Phosphorylation of steroidogenic acute regulatory protein (StAR) modulates its steroidogenic activity. *J. Biol. Chem.* **272,** 32656–32662
17. Dyson, M. T., Jones, J. K., Kowalewski, M. P., Manna, P. R., Alonso, M., Gottesman, M. E., and Stocco, D. M. (2008) Mitochondrial A kinase anchoring protein 121 binds type II protein kinase A and enhances steroidogenic acute regulatory protein-mediated steroidogenesis in MA-10 mouse Leydig tumor cells. *Biol. Reprod.* **78,** 267–277
18. Jo, Y., King, S. R., Khan, S. A., and Stocco, D. M. (2005) Involvement of protein kinase C and cyclic adenosine 3',5'-monophosphate-dependent kinase in steroidogenic acute regulatory protein expression and steroid biosynthesis in Leydig cells. *Biol. Reprod.* **73,** 244–255
19. Fleury, A., Mathieu, A. P., Ducharme, L., Hales, D. B., and LeHoux, J. G. (2004) Phosphorylation and function of the hamster adrenal steroidogenic acute regulatory protein (StAR). *J. Steroid Biochem. Mol. Biol.* **91,** 259–271
20. Bose, M., Whittal, R. M., Miller, W. L., and Bose, H. S. (2008) Steroidogenic activity of StAR requires contact with mitochondrial VDAC1 and phosphate carrier protein. *J. Biol. Chem.* **283,** 8837–8845
21. Clark, B. J., Soo, S. C., Caron, K. M., Ikeda, Y., Parker, K. L., and Stocco,

D. M. (1995) Hormonal and developmental regulation of the steroidogenic acute regulatory protein. *Mol. Endocrinol.* **9,** 1346–1355
22. Bose, H. S., Whittal, R. M., Baldwin, M. A., and Miller, W. L. (1999) The active form of the steroidogenic acute regulatory protein, StAR, appears to be a molten globule. *Proc. Natl. Acad. Sci. U.S.A.* **96,** 7250–7255
23. Baker, B. Y., Yaworsky, D. C., and Miller, W. L. (2005) A pH-dependent molten globule transition is required for activity of the steroidogenic acute regulatory protein, StAR. *J. Biol. Chem.* **280,** 41753–41760
24. Arakane, F., Sugawara, T., Nishino, H., Liu, Z., Holt, J. A., Pain, D., Stocco, D. M., Miller, W. L., and Strauss, J. F., 3rd (1996) Steroidogenic acute regulatory protein (StAR) retains activity in the absence of its mitochondrial import sequence: implications for the mechanism of StAR action. *Proc. Natl. Acad. Sci. U.S.A.* **93,** 13731–13736
25. Bose, H. S., Lingappa, V. R., and Miller, W. L. (2002) Rapid regulation of steroidogenesis by mitochondrial protein import. *Nature* **417,** 87–91
26. Baker, B. Y., Epand, R. F., Epand, R. M., and Miller, W. L. (2007) Cholesterol binding does not predict activity of the steroidogenic acute regulatory protein, StAR. *J. Biol. Chem.* **282,** 10223–10232
27. Sugawara, T., Lin, D., Holt, J. A., Martin, K. O., Javitt, N. B., Miller, W. L., and Strauss, J. F., 3rd (1995) Structure of the human steroidogenic acute regulatory protein (StAR) gene. StAR stimulates mitochondrial cholesterol 27-hydroxylase activity. *Biochemistry* **34,** 12506–12512
28. Manna, P. R., Eubank, D. W., Lalli, E., Sassone-Corsi, P., and Stocco, D. M. (2003) Transcriptional regulation of the mouse steroidogenic acute regulatory protein gene by the cAMP response element-binding protein and steroidogenic factor 1. *J. Mol. Endocrinol.* **30,** 381–397
29. Lin, D., Sugawara, T., Strauss, J. F., 3rd, Clark, B. J., Stocco, D. M., Saenger, P., Rogol, A., and Miller, W. L. (1995) Role of steroidogenic acute regulatory protein in adrenal and gonadal steroidogenesis. *Science* **267,** 1828–1831
30. Tsujishita, Y., and Hurley, J. H. (2000) Structure and lipid transport mechanism of a StAR-related domain. *Nat. Struct. Biol.* **7,** 408–414
31. Hurley, J. H., Tsujishita, Y., and Pearson, M. A. (2000) Floundering about at cell membranes. A structural view of phospholipid signaling. *Curr. Opin. Struct. Biol.* **10,** 737–743
32. Rosenquist, M., Sehnke, P., Ferl, R. J., Sommarin, M., and Larsson, C. (2000) Evolution of the 14-3-3 protein family. Does the large number of isoforms in multicellular organisms reflect functional specificity? *J. Mol. Evol.* **51,** 446–458
33. Tzivion, G., Shen, Y. H., and Zhu, J. (2001) 14-3-3 proteins. Bringing new definitions to scaffolding. *Oncogene* **20,** 6331–6338
34. Aitken, A. (2006) 14-3-3 proteins. A historic overview. *Semin. Cancer Biol.* **16,** 162–172
35. Hachiya, N., Komiya, T., Alam, R., Iwahashi, J., Sakaguchi, M., Omura, T., and Mihara, K. (1994) MSF, a novel cytoplasmic chaperone that functions in precursor targeting to mitochondria. *EMBO J.* **13,** 5146–5154
36. Ichimura, T., Ito, M., Itagaki, C., Takahashi, M., Horigome, T., Omata, S., Ohno, S., and Isobe, T. (1997) The 14-3-3 protein binds its target proteins with a common site located toward the C terminus. *FEBS Lett.* **413,** 273–276
37. Toker, A., Sellers, L. A., Amess, B., Patel, Y., Harris, A., and Aitken, A. (1992) Multiple isoforms of a protein kinase C inhibitor (KCIP-1/14-3-3) from sheep brain. Amino acid sequence of phosphorylated forms. *Eur. J. Biochem.* **206,** 453–461
38. Xiao, B., Smerdon, S. J., Jones, D. H., Dodson, G. G., Soneji, Y., Aitken, A., and Gamblin, S. J. (1995) Structure of a 14-3-3 protein and implications for coordination of multiple signaling pathways. *Nature* **376,** 188–191
39. Liu, D., Bienkowska, J., Petosa, C., Collier, R. J., Fu, H., and Liddington, R. (1995) Crystal structure of the ζ isoform of the 14-3-3 protein. *Nature* **376,** 191–194
40. Ganguly, S., Weller, J. L., Ho, A., Chemineau, P., Malpaux, B., and Klein, D. C. (2005) Melatonin synthesis. 14-3-3-Dependent activation and inhibition of arylalkylamine *N*-acetyltransferase mediated by phosphoserine-205. *Proc. Natl. Acad. Sci. U.S.A.* **102,** 1222–1227
41. Johnson, C., Crowther, S., Stafford, M. J., Campbell, D. G., Toth, R., and MacKintosh, C. (2010) Bioinformatic and experimental survey of 14-3-3 binding sites. *Biochem. J.* **427,** 69–78
42. Muslin, A. J., Tanner, J. W., Allen, P. M., and Shaw, A. S. (1996) Interaction of 14-3-3 with signaling proteins is mediated by the recognition of phosphoserine. *Cell* **84,** 889–897
43. Hauet, T., Yao, Z. X., Bose, H. S., Wall, C. T., Han, Z., Li, W., Hales, D. B., Miller, W. L., Culty, M., and Papadopoulos, V. (2005) Peripheral-type benzodiazepine receptor-mediated action of steroidogenic acute regulatory protein on cholesterol entry into Leydig cell mitochondria. *Mol. Endocrinol.* **19,** 540–554
44. Li, H., Yao, Z., Degenhardt, B., Teper, G., and Papadopoulos, V. (2001) Cholesterol binding at the cholesterol recognition/interaction amino acid consensus (CRAC) of the peripheral-type benzodiazepine receptor and inhibition of steroidogenesis by an HIV TAT-CRAC peptide. *Proc. Natl. Acad. Sci. U.S.A.* **98,** 1267–1272
45. Yaffe, M. B., Rittinger, K., Volinia, S., Caron, P. R., Aitken, A., Leffers, H., Gamblin, S. J., Smerdon, S. J., and Cantley, L. C. (1997) The structural basis for 14-3-3. Phosphopeptide binding specificity. *Cell* **91,** 961–971
46. Jefcoate, C. (2002) High-flux mitochondrial cholesterol trafficking, a specialized function of the adrenal cortex. *J. Clin. Invest.* **110,** 881–890
47. Liu, J., Li, H., and Papadopoulos, V. (2003) PAP7, a PBR/PKA-RIα-associated protein. A new element in the relay of the hormonal induction of steroidogenesis. *J. Steroid Biochem. Mol. Biol.* **85,** 275–283
48. Liu, J., Rone, M. B., and Papadopoulos, V. (2006) Protein-protein interactions mediate mitochondrial cholesterol transport and steroid biosynthesis. *J. Biol. Chem.* **281,** 38879–38893
49. Dalal, S. N., Schweitzer, C. M., Gan, J., and DeCaprio, J. A. (1999) Cytoplasmic localization of human cdc25C during interphase requires an intact 14-3-3 binding site. *Mol. Cell. Biol.* **19,** 4465–4479
50. Eilers, A. L., Sundwall, E., Lin, M., Sullivan, A. A., and Ayer, D. E. (2002) A novel heterodimerization domain, CRM1, and 14-3-3 control subcellular localization of the MondoA-Mlx heterocomplex. *Mol. Cell. Biol.* **22,** 8514–8526
51. Liu, M. Y., Cai, S., Espejo, A., Bedford, M. T., and Walker, C. L. (2002) 14-3-3 interacts with the tumor suppressor tuberin at Akt phosphorylation site(s). *Cancer Res.* **62,** 6475–6480
52. Lee, J. H., and Lu, H. (2011) 14-3-3γ inhibition of MDMX-mediated p21 turnover independent of p53. *J. Biol. Chem.* **286,** 5136–5142
53. Radhakrishnan, V. M., and Martinez, J. D. (2010) 14-3-3γ induces oncogenic transformation by stimulating MAP kinase and PI3K signaling. *PLoS One* **5,** e11433
54. Yacoubian, T. A., Slone, S. R., Harrington, A. J., Hamamichi, S., Schieltz, J. M., Caldwell, K. A., Caldwell, G. A., and Standaert, D. G. (2010) Differential neuroprotective effects of 14-3-3 proteins in models of Parkinson disease. *Cell Death. Dis.* **1,** e2
55. Bridges, D., and Moorhead, G. B. (2005) 14-3-3 proteins. A number of functions for a numbered protein. *Sci. STKE. 2005*, re10
56. Brown, A. S., Hall, P. F., Shoyab, M., and Papadopoulos, V. (1992) Endozepine/diazepam binding inhibitor in adrenocortical and Leydig cell lines. Absence of hormonal regulation. *Mol. Cell. Endocrinol.* **83,** 1–9
57. Aitken, A. (2002) Functional specificity in 14-3-3 isoform interactions through dimer formation and phosphorylation. Chromosome location of mammalian isoforms and variants. *Plant Mol. Biol.* **50,** 993–1010
58. Aitken, A., Baxter, H., Dubois, T., Clokie, S., Mackie, S., Mitchell, K., Peden, A., and Zemlickova, E. (2002) Specificity of 14-3-3 isoform dimer interactions and phosphorylation. *Biochem. Soc. Trans.* **30,** 351–360
59. Shen, Y. H., Godlewski, J., Bronisz, A., Zhu, J., Comb, M. J., Avruch, J., and Tzivion, G. (2003) Significance of 14-3-3 self-dimerization for phosphorylation-dependent target binding. *Mol. Biol. Cell* **14,** 4721–4733
60. Alpy, F., and Tomasetto, C. (2005) Give lipids a START. The StAR-related lipid transfer (START) domain in mammals. *J. Cell Sci.* **118,** 2791–2801
61. Rittinger, K., Budman, J., Xu, J., Volinia, S., Cantley, L. C., Smerdon, S. J., Gamblin, S. J., and Yaffe, M. B. (1999) Structural analysis of 14-3-3 phosphopeptide complexes identifies a dual role for the nuclear export signal of 14-3-3 in ligand binding. *Mol. Cell* **4,** 153–166
62. Hartung, S., Rust, W., Balvers, M., and Ivell, R. (1995) Molecular cloning and *in vivo* expression of the bovine steroidogenic acute regulatory protein. *Biochem. Biophys. Res. Commun.* **215,** 646–653
63. Martens, G. J., Piosik, P. A., and Danen, E. H. (1992) Evolutionary conservation of the 14-3-3 protein. *Biochem. Biophys. Res. Commun.* **184,**

1456–1459
64. Alam, R., Hachiya, N., Sakaguchi, M., Kawabata, S., Iwanaga, S., Kitajima, M., Mihara, K., and Omura, T. (1994) cDNA cloning and characterization of mitochondrial import stimulation factor (MSF) purified from rat liver cytosol. *J. Biochem.* **116,** 416–425
65. Hachiya, N., Alam, R., Sakasegawa, Y., Sakaguchi, M., Mihara, K., and Omura, T. (1993) A mitochondrial import factor purified from rat liver cytosol is an ATP-dependent conformational modulator for precursor proteins. *EMBO J.* **12,** 1579–1586
66. Hachiya, N., Mihara, K., Suda, K., Horst, M., Schatz, G., and Lithgow, T. (1995) Reconstitution of the initial steps of mitochondrial protein import. *Nature* **376,** 705–709
67. Mathieu, A. P., Lavigne, P., and LeHoux, J. G. (2002) Molecular modeling and structure-based thermodynamic analysis of the StAR protein. *Endocr. Res.* **28,** 419–423
68. Mathieu, A. P., Fleury, A., Ducharme, L., Lavigne, P., and LeHoux, J. G. (2002) Insights into steroidogenic acute regulatory protein (StAR)-dependent cholesterol transfer in mitochondria. Evidence from molecular modeling and structure-based thermodynamics supporting the existence of partially unfolded states of StAR. *J. Mol. Endocrinol.* **29,** 327–345